SUPPORTING INFORMATION

Nonspherical Coacervate Shapes in an Enzyme-Driven Active System

Willem Kasper Spoelstra[1], Eli O. van der Sluis[1], Marileen Dogterom[1]*, Louis Reese[1]*

[1]Department of Bionanoscience, Kavli Institute of Nanoscience Delft, Delft University of Technology, Delft, The Netherlands

*To whom correspondence should be addressed: M.Dogterom@tudelft.nl & louisreese@protonmail.com

TABLE OF CONTENTS

Gel electrophoresis assay

To establish that PNPase indeed polymerizes poly$(U)_{20}$ by adding UMP from UDP, we ran a gel electrophoresis assay. 5 µM Cy5-labeled poly$(U)_{20}$ and 40 mM UDP were mixed in 1x PNPase synthesis buffer (100 mM Tris-HCl, 1 mM EDTA, 5 mM $MgCl_2$, pH 9.0, without and with 1.0 wt% spermine). Then ~1 µM PNPase was added and every 10 minutes a fraction was frozen in liquid nitrogen and stored at -80 °C. The reaction was kept at 30 °C. Samples were quickly thawed in hand, mixed with 2x RNA loading dye (NEB), heated to 70 °C for 10 minutes and ran on a 1% agarose gel (**Fig. S1**). To visualize the ladder (Riboruler High Range RNA Ladder, Thermo Fischer), the gel was pre-stained with 1x SYBR Safe (Thermo Fischer).

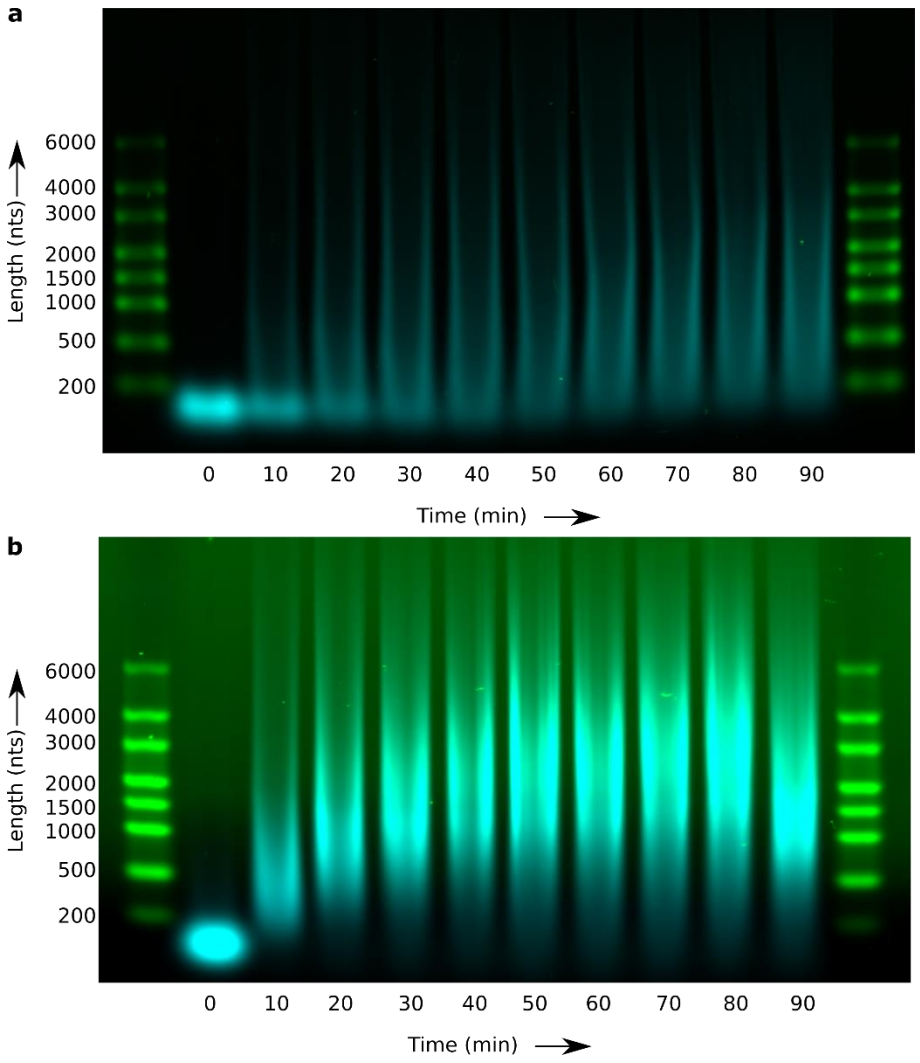

Figure S1: Gel electrophoresis assay displaying poly(U)-polymerization by PNPase. Gel electrophoresis image with the RNA polymerization by PNPase without (a) and with (b) 1.0 wt% spermine. RNA under polymerization contained a Cy5-label at the 5'-end (cyan). SYBR Safe stained RiboRuler High Range RNA Ladder was added in the outer lanes (green) to rotate the image for alignment. The images are false-colored and rescaled to enhance visibility.

3D images of coacervates sedimented onto PVA-coated slide

To test the wetting behavior of the coacervates on the polyvinyl alcohol (PVA) coated glass slides, we acquired Z-stacks of both passive and active coacervates (**Fig. S2**). We observed that the passive coacervates were spherical and did not wet the PVA-coated glass coverslip on which they sedimented (**Fig. S2a & b**). Active coacervates also did not wet the PVA-coated glass coverslip (**Fig. S2c-e**).

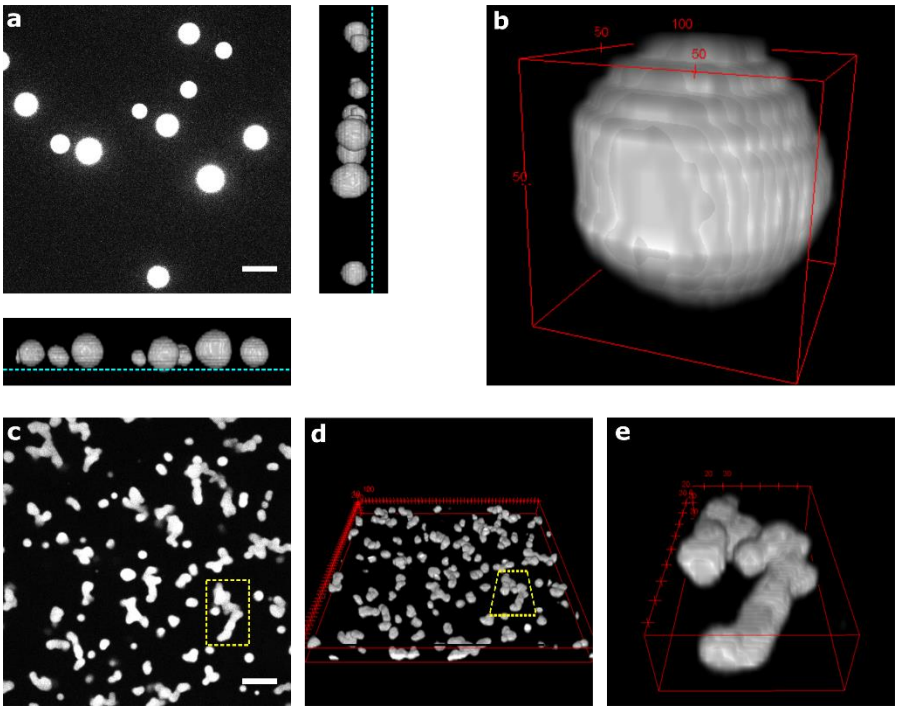

Figure S2: 3D imaging of coacervates on PVA coated glass surface. (a) Passive coacervates sedimented onto a PVA-coated glass coverslip were spherical and did not wet the surface (cyan dashed lines in bottom and side views). (b) 3D reconstruction of single spherical coacervate sedimented onto the PVA-coated glass coverslip. (c) Non-spherical active coacervates formed by PNPase. (d) 3D reconstruction of the non-spherical coacervates shown in panel c. (e) 3D reconstruction of the single non-spherical coacervate highlighted by the yellow dashed squares in panels c and d. Scale bars in panels a and c represent 10 μm. 3D reconstructions of Z-stack images were made using the 3D viewer plugin in ImageJ[1].

Theoretical considerations for circularity-based quantification

Here we provide the rationale behind using circularity of cross sections as a measure of how far non-spherical coacervates are away from their spherical equilibrium shape. The Gibbs free energy associated with a liquid-liquid interface is proportional to interfacial surface area[2]:

$$G_{interface} = \gamma A_{interface}$$

Where $\gamma = \left(\frac{\partial G}{\partial A}\right)_{T,P,n}$ denotes the interfacial tension between the two coexisting liquid phases. For a three-dimensional body of volume V and surface area S, the sphericity Ψ is defined as the surface area of a sphere with volume V over the actual surface area of the body:

$$\Psi = \frac{\sqrt[3]{\pi} \cdot (6V)^{2/3}}{S}$$

Sphericity is thus a non-dimensional measure of how close a body resembles a sphere, and takes on values between 0 and 1. Sphericity of 0 implies a infinitely long and thin rod, and sphericity of 1 implies a perfect sphere. From combining equations for $G_{interface}$ and Ψ, we find that the Gibbs free energy in units of surface area is inversely proportional to the sphericity:

$$\frac{G_{interface}}{V^{2/3}} \propto \frac{1}{\Psi}$$

To relate the Gibbs free energy of coacervate-solvent interfaces directly to the shape requires a full 3D coacervate structure. Because it is not possible to deduce the full 3D coacervate structure from the 2D images acquired under the confocal microscope, we instead looked at the circularity ϑ, which is a 2D analog of sphericity. It is defined as 4π times the ratio between the area A of a 2D-object, over its perimeter (P) squared

$$\vartheta = \frac{4\pi A}{P^2}$$

as described in the main text. A circularity of $\vartheta = 0$ infinitely thin line, whereas $\vartheta = 1$ implies a perfect circle. The Gibbs free energy of a 2D thin slice of liquid-liquid interface would be proportional to the perimeter:

$$G^{2D} = \gamma P$$

Combining the expressions for G^{2D} and ϑ now yields the following relation between "two-dimensional" Gibbs free energy and the circularity of an object.

$$\frac{G^{2D}}{A^{1/2}} \propto \frac{1}{\sqrt{\vartheta}}$$

The two-dimensional Gibbs free energy per unit interface is thus inversely proportional to $\sqrt{\vartheta}$. Therefore in our context, we use $\sqrt{\vartheta}$ as the 2D analog of Ψ. Note that the square root of the circularity bears no physical significance, as it remains 0 for infinitely long lines and 1 for perfect circles. Despite the fact that it is not possible to directly relate ϑ to the (three-dimensional) Gibbs free energy of liquid-liquid interfaces, we conclude that the average circularity of 2D slices of coacervates may be interpreted as a relative measure for how far coacervates are from their spherical equilibrium shape.

Number of coacervates in circularity assay

In **Figure S3** the number of coacervates (panels a-c) and the average size of their cross sections (panels d-f) are displayed for the experiments shown in **Figure 2d-f**.

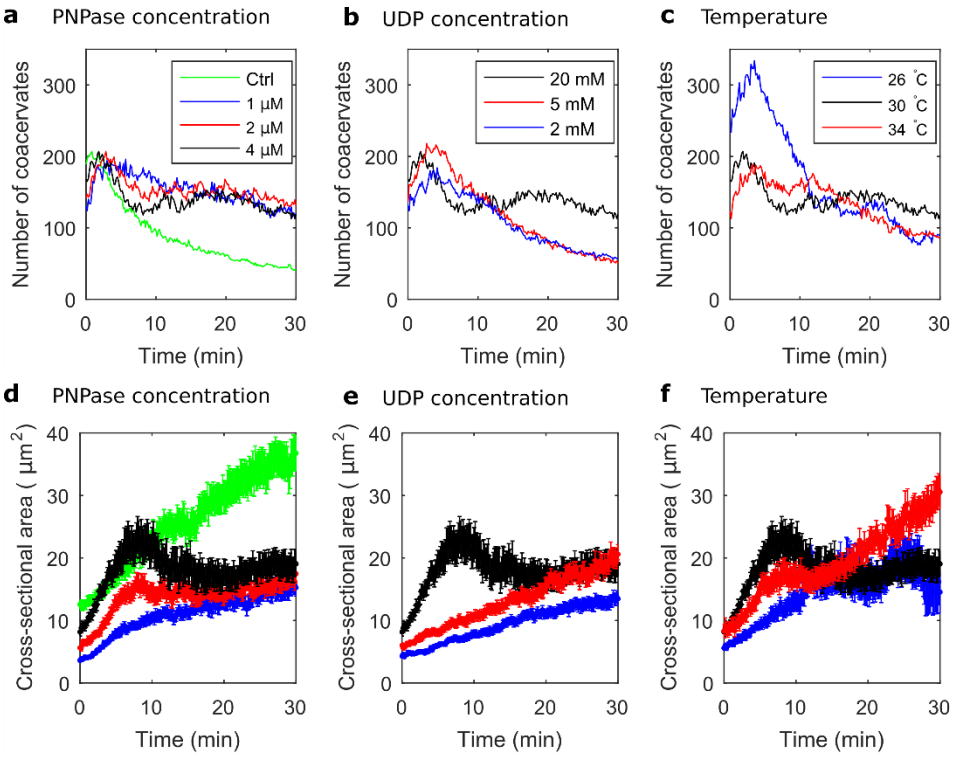

Figure S3: Statistics of coacervates analyzed in Figure 2d-f. (a) Number of coacervates used to calculate the average circularity over time (**Fig. 2d**). The control (green line) represents passive poly(U)$_{\infty}$/spermine coacervates. (b) Number of coacervates used to calculate the circularity of coacervates under different UDP concentrations (**Fig. 2e**). (c) Number of coacervates analyzed to calculate the average circularity at different temperatures (**Fig. 2f**). (d) Average cross-sectional area of coacervates used to calculate the average circularity over time (**Fig. 2d**). (e) Average cross-sectional area of coacervates used to calculate the circularity of coacervates under different UDP concentrations (**Fig. 2e**). (f) Average cross-sectional area of coacervates analyzed to calculate the average circularity at different temperatures (**Fig. 2f**). Error bars indicate standard error from the mean (n = 3 per condition). The legends of panels a-c apply to d-f, respectively.

Data processing and Supporting Information of CRAM analysis

Merging events were cropped and binarized as described in the **Materials & Methods** (**Fig. S4a & b**). In total, we analyzed 53 merging events of coacervates with comparable size. From the definition of circularity and a simple geometric argument it is clear that two spheres of same radius should give $a = 1$ and $a - b = \frac{1}{2}$ (see **Fig. S4c)**. Due to asymmetries and limited resolution, we obtained $a = 0.91 \pm 0.018$ and $(a - b) = 0.50 \pm 0.11$ (mean ± s.d., n = 53) (**Fig. S4d**).

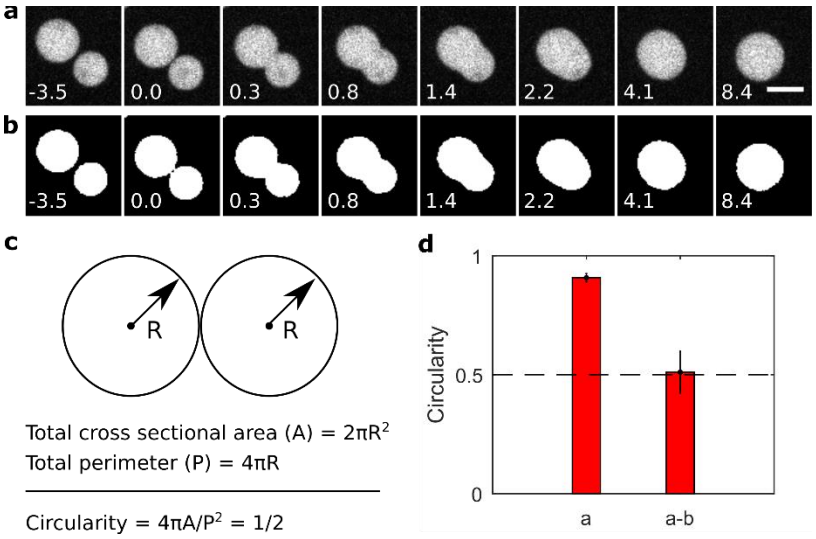

Figure S4: Data processing and statistics of CRAM-analysis. (a) Cropped images of a merging event. (b) Binarized images of the merging event shown in panel a. (c) Illustration of the geometric argument that shows $a = 1$ and $(a - b) = \frac{1}{2}$ for a symmetric merging event of two perfectly spherical and equal-sized coacervates. (d) Average values of fitting parameters a and $(a - b)$ obtained through our analysis. Error bars indicate standard deviation (n = 53).

Purification and chemical labelling of PNPase from *Synechocystis sp* PCC6803

For the localization studies of PNPase in RNA/spermine coacervates, PNPase was purified and chemically labeled. PNPase from *Synechocystis* s*p* PCC6803 was expressed from pET20b-PNP transformed into BL21(DE3)/pLysS cells. Cells were grown at 30 °C in two litres of Magic Media (Invitrogen) supplemented with 100 µg/ml ampicillin and 34 µg/ml chloramphenicol. Cells were harvested (8 min 4500 rpm, JLA8.1000 rotor), washed in 1x PBS buffer and lysed using a French Press (Constant Systems) at 20 kpsi, 4°C. Unbroken cells, debris and aggregates were pelleted in a Ti45 rotor (30 min, 40.000 rpm, 4°C). The lysate was loaded onto a 5 ml Talon column (Clontech) equilibrated with buffer A (20 mM Tris-HCl pH 7.5, 500 mM NaCl, 0.01% Tween 20, 1 mM β-mercaptoethanol), the column was washed extensively with buffer A and PNPase was eluted with a linear gradient to buffer B (20 mM Tris-HCl pH 7.5, 100 mM NaCl, 200 mM imidazol, 1 mM β-mercaptoethanol). Peak fractions were pooled and diluted 4-fold with buffer QA (50 mM Tris/HCl pH 7.5, 5% glycerol, 1 mM β-mercaptoethanol) loaded onto a 1 ml Q-FF column (GE Healthcare) and eluted with a linear gradient to buffer QB (=QA + 1 M NaCl). PNPase was labelled with fluorescein (FITC) while bound to the Q-FF column, by first washing the column with buffer QC (20 mM Tris/HCl pH 7.0, 10 mM NaCl, 5% glycerol), followed by a 30 minute incubation with 0.1 mM fluorescein-5-maleimide in QC at room temperature. Fluorescein-labelled PNPase was eluted as described above. Finally, purified PNPase was desalted using a HiPrep 26/10 column (GE Healthcare) pre-equilibrated with storage buffer: 20 mM HEPES/KOH pH 7.9, 0.1 mM EDTA, 2 mM β-mercaptoethanol, 12.5 mM $MgCl_2$, 60 mM KCl and 20% (w/v) glycerol. The final sample was aliquoted, snap frozen in liquid nitrogen and stored at -80°C.

Aggregation of FITC-PNPase at the coacervate-solvent interface

Imaging of active coacrevates with FITC-labeled PNPase showed FITC-PNPase aggregates which predominantly localized at the coacervate solvent interface (**Fig. S5**). To more accurately quantify the localization of solubilized FITC-PNPase, we clarified the solution prior to UDP addition by ultracentrifugation (Airfuge, 5 min, 30 psi, approx. 100,000g). Although this additional step did not remove all aggregates, it significantly decreased their presence, and also their contribution to the fluorescence intensities.

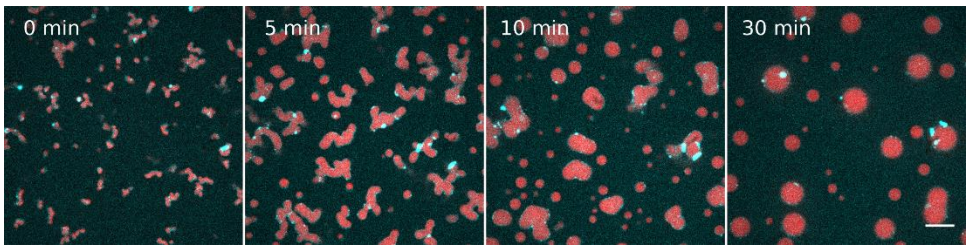

Figure S5: FITC-PNPase forms aggregates which localize to the coacervate-solvent interface. Fluorescence intensities captured from Cy5-poly(U) and FITC-PNPase are displayed in red and cyan respectively.

Quantification of FITC-PNPase localization

Here we describe the image processing and calculations in greater detail, which were employed to obtain the quantification of the PNPase localization inside the coacervate phase (CP), solvent phase (SP) and at the interface. We started from a micrograph time series of the PNPase reaction with FITC-PNPase and Cy5-poly(U) seeds (**Materials & Methods**). First, micrographs acquired by capturing Cy5-poly(U) fluorescence (red) were binarized by smoothing and thresholding using ImageJ (default settings). The binary image was inverted and the edges were identified. In this way three masks were generated, for the solvent phase, for the coacervate phase and for the interface between the two phases. The masks were multiplied with the FITC-PNPase fluorescence micrographs. The resulting images served to calculate the average intensities (using MATLAB R2016a). Black pixels (zero intensity) were omitted by setting them to NaN-valued pixels. The workflow described here is schematically shown in **Figure S6a**. To determine the background fluorescence intensities, we repeated this whole workflow with a time series of Cy5-poly$(U)_{20}$/spermine coacervates in the absence of FITC-PNPase. The average intensities obtained from this control were subtracted from the average FITC-PNPase intensities to obtain **Figure S6b& c**.

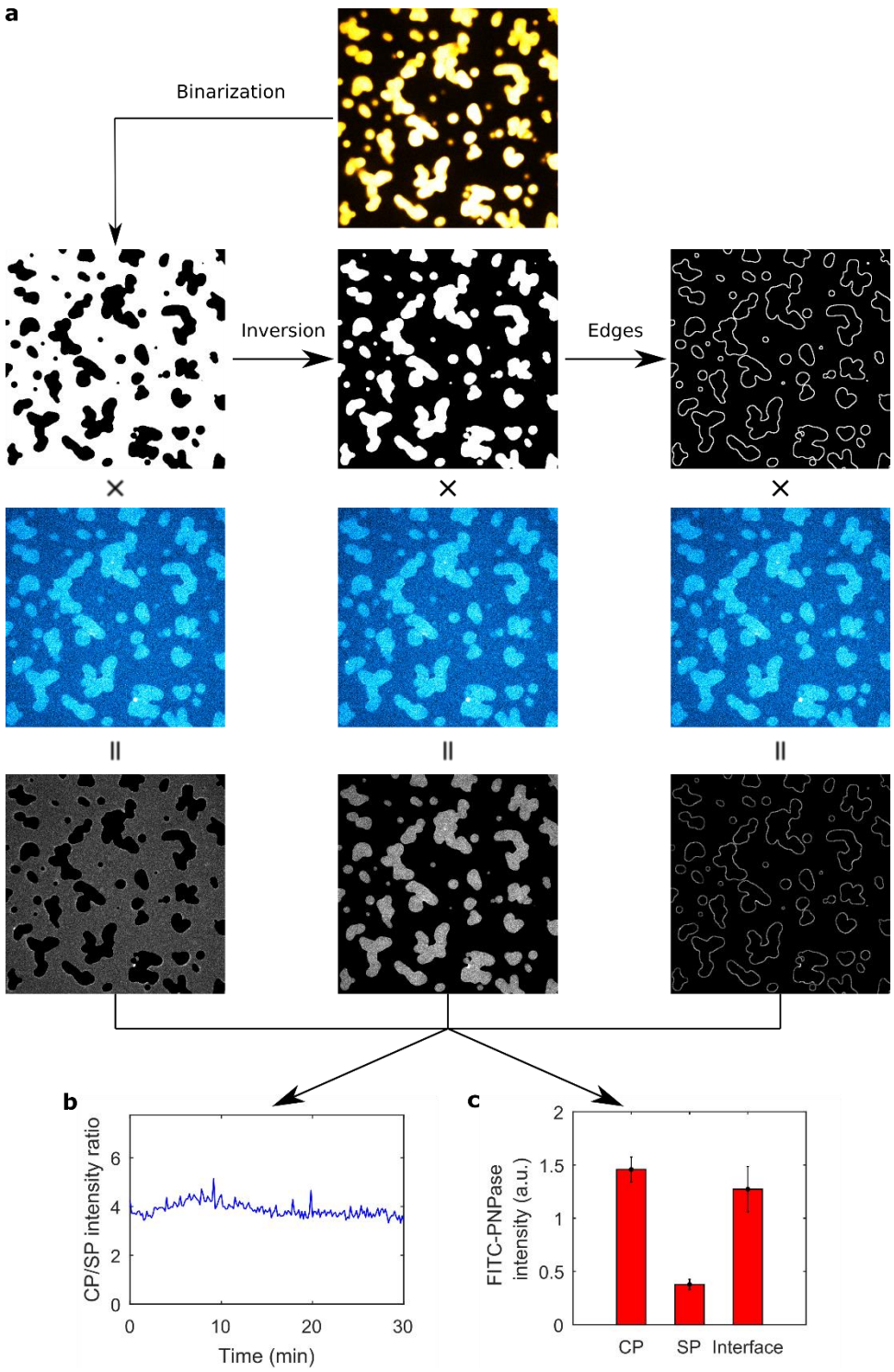

Figure S6: Workflow of image processing for quantification of the PNPase localization. (a) A schematic of the workflow used to quantify PNPase partitioning in the coacervate and solvent phase, and at their interface. Colors are added as a visual aid (red for Cy5-poly(U), cyan for FITC-PNPase). (b)

Fluorescence intensity ratio between CP and SP remained roughly constant over time. On average, this ratio was 3.9 ± 0.6 (mean ± s.d.). (c) Fluorescence intensities of FITC-PNPase in the CP, SP and at their interface.

Analysis of RNA redistribution during merging

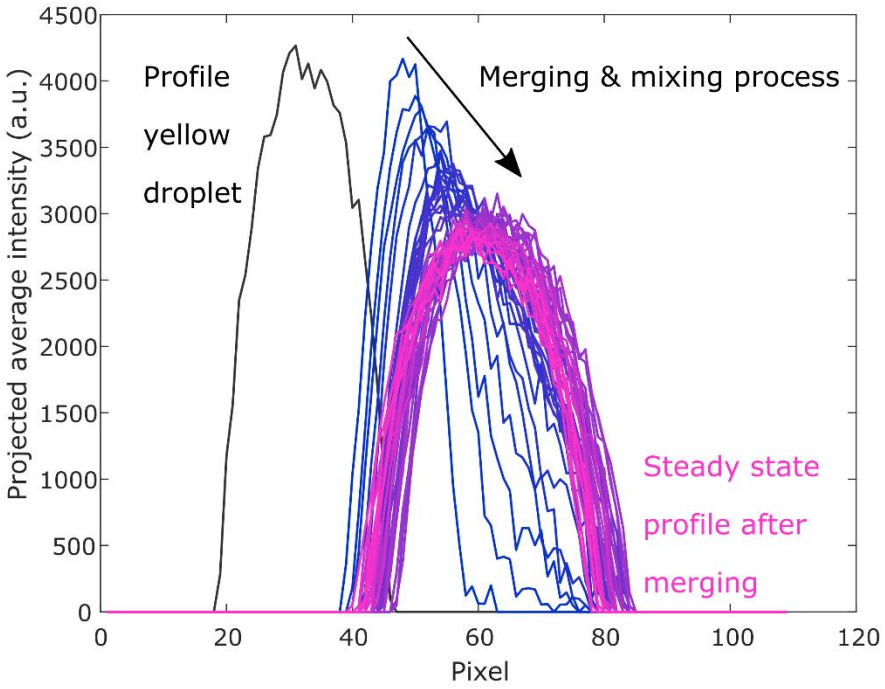

Figure S7: Analysis of timeseries from Figure 3d. We used Fiji to create a binary mask for the droplet shown in yellow in **Fig. 3d**, and then used Matlab to extract the data in the following way: we rotated the image such that the merging interface was vertical. Then, we projected the average intensity of the product between the mask and the original yellow channel over time. The color code from blue to pink indicates progress of time. As expected, fluorophores redistribute towards a lower average intensity in the merged droplet.

Supporting Videos

Supporting Video 1:

Passive poly(U)$_\infty$/spermine coacervates. These coacervates were among the ones used as a control for circularity of passive coacervates (**Fig. 2d, green dots**).

Supporting Video 2:

Poly(U)/spermine coacervates activated by 1 μM PNPase and 20 mM UDP at 30 °C.

Supporting Video 3:

Poly(U)/spermine coacervates activated by 4 μM PNPase and 20 mM UDP at 30 °C.

Supporting Video 4:

Merging of two coacervates formed with Cy3-poly(U) and Cy5-poly(U) (**Fig. 3d**).

References

(1) Schmid, B.; Schindelin, J.; Cardona, A.; Longair, M.; Heisenberg, M. A High-Level 3D Visualization API for Java and ImageJ. *BMC Bioinformatics* **2010**, *11* (274), 1–7.

(2) Doi, M. *Soft Matter Physics*; Oxford University Press, 2013.